water

MDPI

Article

Hydraulic Planning in Insular Urban Territories: The Case of Madeira Island—São João Stream, Funchal, Portugal

Sérgio Lousada [1,2,3,4,5,*], Raul Alves [6], Mário Fernandes [1,7] and Leonardo Gonçalves [1]

1 Department of Civil Engineering and Geology (DECG), Faculty of Exact Sciences and Engineering (FCEE), University of Madeira (UMa), 9000-082 Funchal, Portugal; ptsmario2001@gmail.com (M.F.); leonardobazilio13@gmail.com (L.G.)
2 CITUR—Madeira—Research Centre for Tourism Development and Innovation, 9000-082 Funchal, Portugal
3 VALORIZA—Research Centre for Endogenous Resource Valorization, Polytechnic Institute of Portalegre (IPP), 9000-082 Portalegre, Portugal
4 Research Group on Environment and Spatial Planning (MAOT), University of Extremadura, 06071 Badajoz, Spain
5 RISCO—Civil Engineering Department, University of Aveiro, 3810-193 Aveiro, Portugal
6 Machico City Council (CMM), Largo do Município Machico, 9200-099 Machico, Portugal; raul@cm-machico.pt
7 Faculty of Economics, University of Porto (FEP), 4200-464 Porto, Portugal
* Correspondence: slousada@staff.uma.pt; Tel.: +351-963-611-712

Abstract: This study's primary goal was to conduct an analysis regarding the flood susceptibility of the main watercourse of the São João (Funchal) drainage basin. In addition, if proven necessary, we also aimed to suggest mitigation measures, such as sizing a detention basin and promoting adjustments of the riverbed's roughness coefficient. This study also resorted to geomorphological data—obtained during the watershed characterization process—that were then utilized in the SIG ArcGIS software, in order to estimate the expected peak flow rate, considering a return period of 100 years using the Gumbel distribution. Finally, the Manning–Strickler equation was utilized to determine the river discharge point's drainage capacity; the reason for that was to verify whether its drainage capacity was sufficient to drain the entire volume of rainwater associated with an extreme flood event. In summary, the results obtained by this study indicate that the drainage capacity of the river discharge point of the São João watershed (Funchal) is insufficient when considering an extreme flood event, for a return period of 100 years. Hence, it became necessary to explore the two aforementioned mitigation measures: first, regarding the detention basin, its sizing was calculated through both the Dutch method and the simplified triangular hydrograph method; second, aiming to increase the drainage capacity of the river discharge point, it is suggested that the roughness coefficient should also be modified.

Keywords: hydraulics; hydrology; insular territories; spatial analysis; territorial management; urban planning

Citation: Lousada, S.; Alves, R.; Fernandes, M.; Gonçalves, L. Hydraulic Planning in Insular Urban Territories: The Case of Madeira Island—São João Stream, Funchal, Portugal. *Water* **2023**, *15*, 2075. https://doi.org/10.3390/w15112075

Academic Editor: Renato Morbidelli

Received: 24 April 2023
Revised: 19 May 2023
Accepted: 22 May 2023
Published: 30 May 2023

1. Introduction

It has become a consensus that climate change is directly connected with the increase in the periodicity of natural disasters. The effects related to climate change are projected to intensify over the course of the 21st century and even beyond, with all of the potential associated negative impacts [1]. The frequency of extreme weather events—e.g., strong rainstorms that cause floods across the world—has been increasing, mostly due to climate change. Because of the rising temperatures that result from global warming, climate change has become a significant menace to the hydrological cycle of river catchments. Indeed, global warming is related to disturbances of precipitation's intensity and frequency, considering certain climatic conditions [2,3]. Moreover, climate change also affects the hydrological cycle in various ways, namely, by modifying peak flows and volumes [4–8].

In the coming years, floods are projected to become some of the most frequent natural disasters, not only due to climate change, but also because of human activities. Every year, millions of people across the world end up being affected by flooding, as this phenomenon is one of the most costly and destructive types of natural disaster [9]. Due to the registered increase in rainfall's intensity and frequency, floods have recently become more recurrent and intense events [10,11]. As a matter of fact, in the past few decades, floods have had the most significant effects on people, territory, and socioeconomic assets among the most frequent natural disasters [12,13].

In recent years, the urbanization process has been accelerating globally [14–16]. Currently, over 50% of the world's inhabitants reside in urbanized regions. Moreover, the part of the world population that resides in these areas is expected to increase by 2.5 billion between 2018 and 2050, with the majority of this projected growth occurring in Asia and Africa [15,16]. As a consequence of such a scenario, challenges for policymakers are expected to arise—mostly regarding the allocation of resources [16]. Thus, this growing wave of urbanization, in addition to extreme rains that have recently taken place, is believed to be leading to an enhancement in terms of the periodicity and impact of flash floods all over the globe [10,17]. Therefore, flood frequency is expected to rise, alongside the number of individuals that might end up being affected by this phenomenon—in part because of the acceleration of urbanization and climate change. Additionally, in recent decades, there has been an increase in the level of vulnerability associated with coastal areas and floodplains—regions where socioeconomic activities tend to be concentrated. Hence, the effects of flooding events have become more severe due to the consequences of climate change and the concentration of socioeconomic activities in regions where the risk of flooding is considerably high [13,18]. Despite climate change contributing to more elevated levels of river flows—which, ultimately, lead to a higher risk of flooding—this factor must not be considered the sole cause of more frequent and intense flooding events. Indeed, the risk of flooding can be influenced by multiple factors, with non-climatic factors—namely, alterations in the catchment area and the process of urbanization—being extremely relevant as well [9,19–21].

Notwithstanding the substantial progress that has occurred in terms of flood risk management [22–24], and in extreme rainfall and flood forecasting and warning systems [25,26], recent floods have still managed to cause significant human casualties around the world [27–30]. The continuous socioeconomic growth may significantly amplify the impacts of floods in the coming decades [31,32]. Furthermore, floods are considered to be among the most catastrophic and recurrent natural disasters, due to the substantial damage and large-scale impacts that they cause within communities [33–35].

Flooding can result in various damages, especially in the fields of agriculture and infrastructure, in addition to the displacement of communities and even the loss of human lives [36,37]. Factors such as climate change and global warming have been cited as relevant contributing factors to heightened and extended rainfall patterns, which can ultimately result in an increase in the recurrence of flooding incidents [33,38]. Nonetheless, the increased impacts that derive from floods could be linked to human-induced aspects, such as rapid population growth, uncontrolled urbanization, and inadequate flood mitigation strategies [39,40]. Of the aforementioned factors, one could point out that ensuring that an efficient and accurate flood management plan is followed is crucial in mitigating the impacts of flooding. Thus, to enhance the current mechanisms of mitigation, it has become imperative to resort to the latest technological advances [40]. An efficient assessment regarding the risks associated with floods is imperative to mitigate the overall impact of these phenomena. As a matter of fact, hydrologists employ the concept of a "design flood", which refers to a flood discharge linked to an average recurrence interval or return period [41,42]. This concept can be utilized in multiple engineering domains—for instance, during the planning and design processes of structures such as bridges, flood control levees, culverts, and drainage pipes. In fact, sustainable flood management finds one of its most important bases in reliable design flood estimation [42].

Thus, considering this framework, meteorological and climatic events and forces have to be seen as pertinent issues. Indeed, the significant levels of instability that exist in the hydrogeological field pose a serious problem—namely, in terms of the effects that they might end up having on the population, socioeconomic activities, infrastructure, and productivity [13]. However, the fact is that floods—like most natural phenomena—cannot be prevented. On the contrary, certain activities carried out by people can, in fact, enhance the impacts of these natural disasters; if one adds climate change to those activities, then not would only the impacts of floods increase, but they would also become more recurrent events. When floods occur, rivers tend to occupy areas that are inherent to their natural course but have been encroached upon by human settlements over the decades. Hence, it is usual for floods to be misclassified as natural disasters, whereas the most accurate classification would be a "calamitous event", given that it affects the population and their activities. The impact that this type of phenomenon has in Madeira, Portugal, is significantly high, which then constitutes a matter of social significance due to the number of human victims and the substantial levels of damage that floods cause to buildings, infrastructure, and industries. In order to ensure that proper management of the land is accomplished, it becomes necessary to conduct a hydrogeological risk assessment, since this allows for the estimation of losses generated by an extreme event, given a certain return period. It is even worth mentioning that this assessment can be expressed either in terms of negative impacts or through the probability of such an event occurring [13,43]. When assessing risk, three aspects need to be considered: hazard (H), vulnerability (V), and exposure (E). With hazard, we point out how likely it is for flooding to occur within a specified timeframe and location. With vulnerability, we refer to the extent of the impact that will affect one or more elements at risk, considering a phenomenon of a certain level of intensity. Finally, with exposure, we refer to the level of harm that could affect multiple elements at risk—e.g., individuals, goods, and real estate. The final result from the combination of these three components can be considered a risk assessment [44].

According to the European Parliament's Directive 2007/60/EC issued on 23 October 2007 [45], regarding the evaluation and control of flood risk, hydraulic studies are necessary for risk assessment. Therefore, there is a requirement to resort to accurate predictive instruments and analytical methodologies in order to identify the real conditions of risk related to the incidence of a given flood event. Regarding urban flood studies, these must provide tools for establishing suitable estimation and prevention strategies. Additionally, flood investigations in urban areas have to consider various aspects, such as the process of gathering topographical data, the characterization of phenomenological processes related to flood currents and their effects on buildings and other structures, and the algorithm selection to solve model equations [46]. Ultimately, these studies must result in graphical outputs—that is, hazard and risk maps. Hence, opting for the correct perspective might be crucial, since graphical results often depend on the author's position when observing reality. When selecting a "point of view", it is important to take multiple factors into account —for instance, the synthesis of the multidimensionality of the features to be represented, the various methodologies that are able to provide a characterization of them, and the representation's purpose. It is worth mentioning that the information from this perspective is particularly important when dealing with environmental emergencies. Moreover, effective risk communication is key to engaging all stakeholders and guaranteeing appropriate management strategies—especially in emergency scenarios [47]. Therefore, presenting the results through virtual scenarios is relevant, as this allows a suitable option to illustrate the conditions that a given region might end up experiencing when a flood takes place. In this case, methodologies must be based on models that accurately depict the hydraulic phenomena, as the images that are generated have to precisely express the computed water surfaces [48]. Multiple mitigation measures could be mentioned when analyzing floods. Those measures can be split into two categories: structural and non-structural. On the one hand, the latter category encompasses mitigation strategies related to the prediction, prevention, and adaptation processes; on the other hand, protective measures tend to be

associated with structural measures, as they often involve engineering structures. However, currently, structural measures are being questioned due to the fact that these structures might end up amplifying the flooding risk and its impact if a failure or breach was to occur; additionally, these measures promote higher levels of vulnerability to these phenomena in flood-prone areas. Hence, non-structural measures are often considered as a viable alternative to lessen flooding's impacts. Examples of non-structural measures can be found in the meteorological and hydrological monitoring processes, land-use planning and regulation, flood hazard and risk mapping, and flood risk and emergency management [45]. A decrease in natural hazards entails various actions, ranging from prevention to emergency management [45,49].

Hence, it is imperative to develop regional studies focused on the flood vulnerability at the basin scale, so as to establish strategies to monitor and manage these events [50].

This study's focus was on conducting a hydrological analysis of the São João watershed (Funchal), with the objective of determining the anticipated peak flow rate, considering a recurrence time of 100 years, and comparing that value with the stream discharge point's drainage capacity. After demonstrating that the discharge point's hydraulic features are not sufficient to ensure that the drainage process is successfully concluded, considering the estimated peak flow rate, it became necessary to estimate the dimensions of a detention basin, aiming to guarantee that the entire flow would be drained and that the stream discharge point would operate normally. Additionally, one of this study's goals was to suggest a structural intervention in this watershed's discharge point—namely, modifying the roughness coefficient associated with the channel's riverbed and walls—without generating significant urban impacts. As a result, the stream's minimum features were assessed to enhance its capacity of drainage without requiring any alterations to its dimensions.

2. Materials and Methods

2.1. Area of Study

The focus of this analysis is the São João watershed (Funchal), which is situated in the Madeira Archipelago—an island group in the North Atlantic, more specifically between latitudes 30°01′ N and 33°08′ N and longitudes 15°51′ W and 17°16′ W [51,52]. More precisely, as presented in Figure 1, the watershed under study belongs to the Funchal municipality and acts as an area of precipitation catchment that ultimately supplies one of the most important streams of this same municipality.

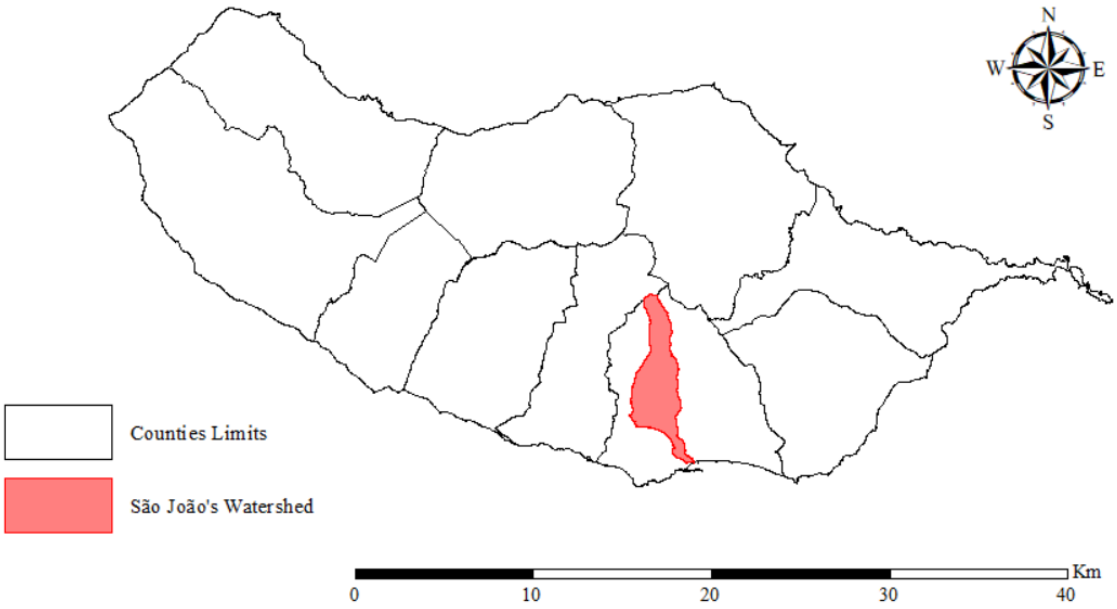

Figure 1. The São João watershed (Funchal). Source: authors, using ESRI ArcGIS, 2020.

Moreover, this watershed has suffered from significant losses due to floods in recent years—namely, in 2010 and 2013. Considering that it is located in an extensively urbanized region, the level of soil sealing is considerably high. Thus, the presence of buildings and pavements in the area of study ends up enhancing the flooding problems that this region experiences [43,53,54]. Furthermore, Figure 2 shows that this watershed's stream discharge point contains sedimentation and vegetation, which contributes to a lower drainage capacity.

Figure 2. State of conservation of São João (Funchal)'s main watercourse river discharge point (from east to river discharge point). Source: authors.

Regarding the level of conservation of this watershed's mainstream, it is mostly uniform in the urbanized areas, which could be simply confirmed in situ. However, the significant amounts of vegetation and sedimentation that are accumulated in the stream might be justified by the stream's reduced slope, which obstructs a rapid drainage process and hampers its ability to drag larger sediments.

2.2. Schematic of the Methodology

As Figure 3 demonstrates, this study's methodology can be divided into 6 different steps.

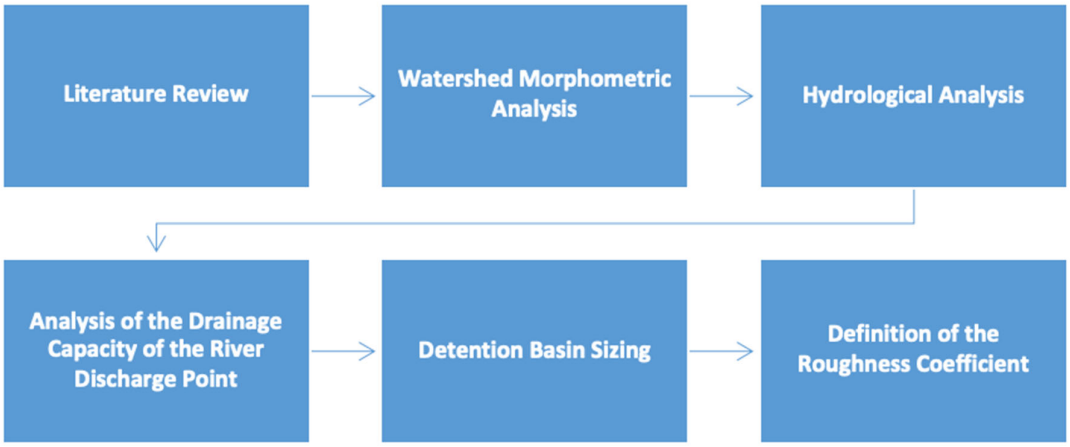

Figure 3. Organogram of the adopted methodology.

In order to conduct an accurate morphometric and hydrological characterization of the watershed under study, it was important to undertake a thorough review of the existing literature in order to ensure that all of the pertinent information would be gathered. After this first step, methodologies suggested by multiple authors were taken into account, aiming to guarantee a satisfactory level of accuracy and reliability for this study. In terms of the remaining steps mentioned in Figure 3, these are described in the next section.

2.3. Morphometric Characterization of the Watershed

Regarding the morphometric characterization of the São João watershed (Funchal), it became necessary to resort to the parameters presented below [55–58]:

- **Gravelius index—K_C:** The relationship between the perimeters of the basin under study and a perfectly circular one—both with identical areas—was utilized to estimate the level of similarity of the watershed's geometric shape to a perfect circle [57]. This parameter can be obtained through Equation (1). As this is a dimensionless parameter, a watershed with a value closer to "1" will have a shape similar to a perfect circle, regardless of its dimensions, which would translate into higher levels of flood propensity [57].

$$K_C = P/\ 2 \times \sqrt{\pi \times A} \quad (1)$$

where
P = the watershed's perimeter (km);
A = the area of the watershed (km^2).

- **Elongation factor—K_L:** The relationship between the watershed being analyzed and a rectangle—both with identical areas—was used to estimate the elongation of the watershed, regardless of its dimensions. This can be determined using Equation (2). If the value obtained for this parameter is higher than "2", then the watershed can be characterized as an elongated one [57].

$$K_L = \frac{L_E}{l_E} = \frac{\frac{K_C \times \sqrt{A}}{1.128} \times \left|1 + \sqrt{1 - \left(\frac{1.128}{K_C}\right)^2}\right|}{\frac{K_C \times \sqrt{A}}{1.128} \times \left|1 - \sqrt{1 - \left(\frac{1.128}{K_C}\right)^2}\right|} \quad (2)$$

where
L_E = equivalent length (km);
l_E = equivalent width (km);
K_C = Gravelius index—a dimensionless parameter;
A = the area of the watershed (km^2).

- **Shape factor—K_F:** This relates the watershed's average length and width. This parameter can be obtained through Equation (3). Lower values are associated with more elongated watersheds and, therefore, with watersheds where the risk of flooding is lower—regardless of their size. Moreover, if the value obtained is "1", then the basin will have a square format.

$$K_F = A/{L_B}^2 \quad (3)$$

where
A = the area of the watershed (km^2);
L_B = the watershed's length (km).

The length of a given watershed might be estimated using the gap that exists between the stream's discharge point and its furthest point. Nonetheless, it is worth mentioning that a watershed's length does not necessarily have to be equal to its main watercourse's length. Some variations between these two values might arise as a result of the larger size that the main watercourse tends to have, mostly because of its sinuosity. By resorting to the MDE file, which was developed by LREC-RAM (the Regional Civil Engineering Laboratory of the Autonomous Region of Madeira), it became feasible to morphologically characterize both the São João watershed (Funchal) and its main channel. In order to avert restrictions associated with using a single method, the data that were gathered during this study were utilized in the equations provided by various authors.

First, to conduct a morphometric analysis, it was necessary to establish a hierarchy based on the order and magnitude of the watercourses; for that reason, both the Strahler and Shreve classifications were utilized [54]. Indeed, these two classifications can be estimated by conducting an analysis based on the DEM file—a process that involves obtaining the "flow direction" and "flow accumulation" rasters through a tool named "flow order" [54]. Additionally, studies have pointed out that the Strahler classification is highly connected with a watershed's ratio of branching/bifurcation. Equation (4) allows for the estimation of each bifurcation degree [43,54,55,57].

$$R_B = \frac{N_i}{N_{i+1}} \quad (4)$$

where
N_i = the number of watercourses labeled as "i"—a dimensionless parameter;
N_{i+1} = the number of watercourses labeled as "i + 1"—a dimensionless parameter.

To obtain this, it is necessary to divide the number of channels of a certain order by the number of channels encompassed in the order immediately above, regardless of their dimensions. Moreover, the average level of bifurcation can be obtained based on Equation (5).

$$\overline{R_B} = \sqrt[i-1]{\prod_{i=1}^{i-1} \frac{N_i}{N_{i+1}}} = \sqrt[i-1]{N_1} \quad (5)$$

where
N_i = the number of watercourses labeled as "i"—a dimensionless parameter;
N_{i+1} = the number of watercourses labeled as "i + 1"—a dimensionless parameter;
N_1 = the number of watercourses of order "1".

As this parameter only denotes the arithmetic mean of the bifurcation ratios, it is also dimensionless. Additionally, a key aspect for an accurate morphometric characterization of any watershed is its concentration time. This parameter indicates the time that the watershed's total area needs to contribute for the drainage process that will culminate in the stream's discharge point [43,54,55,57].

Considering that the methods utilized to calculate the concentration time can be classified as empirical, multiple methodologies might end up producing varying results for the same parameter. Therefore, in order to avoid extreme results, it is advisable to calculate the arithmetic mean. In this case, the arithmetic mean was calculated using the results derived from the methodologies of Kirpich, Témez, and Giandotti (Equations (6)–(8), respectively) [43].

$$t_C = 57 \times \left(L^3/(H_{MAX} - H_{MIN})\right)^{0.385} \quad (6)$$

where
t_C = the concentration time (minutes);
L = the main watercourse's length (km);
H_{MAX} = the main watercourse's maximum height (m);

H_{MIN} = the main watercourse's minimum height (m).

$$t_C = \left(\frac{L}{i^{0.25}}\right)^{0.76} \quad (7)$$

where
t_C = the concentration time (hours);
L = the main watercourse's length (km);
i = the main watercourse's slope (m/m).

$$t_C = \frac{\left(4 + \sqrt{A}\right) + (1.5 \times L)}{0.8 \times \sqrt{H_M}} \quad (8)$$

where
t_C = the concentration time (hours);
A = the area of the watershed (km^2);
L = the main watercourse's length (km);
H_M = the watershed's average height (m).

2.4. Precipitation Analysis

The precipitation analysis that was conducted in this research was based on a probabilistic analysis regarding intense short-term extreme events. To enable this analysis, data were gathered from public sources—including information about precipitation automatically recorded by the National Water Resources Information System (SNIRH). The Gumbel distribution was selected here because it was the probabilistic methodology that would best fit the already-acquired data and the anticipated forecasts for the watersheds located in Madeira [43,54]. Hence, Equation (9) can be utilized to estimate the annual maximum daily precipitation.

$$P_{EST} = P_M + S' \times K_T \quad (9)$$

where
P_{EST} = the estimated maximum daily precipitation, in annual terms (mm);
P_M = the average precipitation, in annual terms (mm);
S' = the standard deviation of the sample (mm);
K_T = the frequency factor—a dimensionless parameter.
where:

$$S' = \left(\frac{\sum(X_i - X_M)^2}{n'}\right)^{0.5} \quad (10)$$

where
X_i = the sample value (mm);
X_M = the sample mean (mm);
n' = the number of samples.

$$K_T = -\frac{6^{0.5}}{\pi} \times \left\{0.577216 + \ln\left(\ln\left(\frac{T_R}{T_R - 1}\right)\right)\right\} \quad (11)$$

where
T_R = the return period (years).

A posteriori, given a certain duration, the intensity of the precipitation can be determined utilizing Equation (12):

$$I = \frac{P_{EST} \times k}{t_C} \quad (12)$$

where
I = the intensity of the precipitation (mm/h);
P_{EST} = the estimated maximum daily precipitation, in annual terms (mm);
t_C = the concentration time (hours);
k = the coefficient of time distribution—a dimensionless parameter.
where:

$$k = 0.181 \times \ln(t_C) + 0.4368 \quad (13)$$

where
t_C = the concentration time (hours).

Given that the annual maximum daily precipitation is applicable only to events that last an entire day, the coefficient of time distribution assumes a key importance. Thus, since a watershed's concentration time is equal to the duration of the precipitation event, if one was to utilize the total level of daily precipitation, it would ultimately result in oversized hydraulic structures [55,57].

2.5. Drainage Capacity of the River Discharge Point and Peak Flow Rate

The Manning–Strickler equation, presented in Equation (14), was utilized to calculate the stream discharge point's drainage capacity; then, we established a comparison between the obtained value and the projected flow considering an extreme event, for a return period of 100 years. Moreover, to estimate the projected flow, multiple methodologies with a significant level of support among researchers were utilized—namely, Forti, Rational, Giandotti, and Mockus (Equations (16)–(19), respectively).

$$Q_M = \left(\frac{1}{n}\right) \times A_M \times R^{\frac{2}{3}} \times \sqrt{i} \quad (14)$$

where
Q_M = the stream discharge point's drainage capacity (m^3/s).
A_M = the area of the river discharge point's cross-section (m^2);
R = the hydraulic radius (m);
i = the river discharge point's slope, in average terms (m/m);
n = the coefficient of roughness of the walls and riverbed ($m^{-1/3}$ s) (Table A1).
where:

$$R = \frac{B + 2 \times h}{A_M} \quad (15)$$

where
B = the stream discharge point runoff section's width (m);
h = the stream discharge point runoff section's height (m);
A_M = the area of the stream discharge point's cross-section (m^2).

It is worth mentioning that previous studies that have focused on this area were used as the main sources to gather information regarding aspects such as the stream's height and width in the discharge point area [57]. In fact, the confirmation of this first parameter was possible due to the utilization of the georeferencing process.

$$Q_{Forti} = A \times \left(b \times \frac{500}{125 + A}\right) + c \quad (16)$$

where
Q_{Forti} = the peak flow rate according to Forti (m^3/s);
A = the area of the watershed (km^2);
b = for this parameter, the value was "2.35" if the maximum daily precipitation level stayed below 200 mm, and "3.25" for levels above 200 mm;
c = for this parameter, the value was "0.5" if the maximum daily precipitation level stayed below 200 mm, and "1" for levels above 200 mm.

$$Q_{Rational} = \frac{C \times I \times A}{3.6} \quad (17)$$

where
$Q_{Rational}$ = the peak flow rate according to the Rational methodology (m^3/s);
C = the coefficient of surface runoff (Table A2);
I = the intensity of the precipitation (mm/h);
A = the area of the watershed (km^2).

$$Q_{Giandotti} = \frac{\lambda \times A \times P_{MAX}}{t_C} \quad (18)$$

where
$Q_{Giandotti}$ = the peak flow rate according to Giandotti (m^3/s);
λ = the reduction coefficient (Table A3);
A = the area of the watershed (km^2);
P_{MAX} = the height of precipitation, considering that the event has a duration identical to the concentration time (mm);
t_C = the concentration time (hours).

$$Q_{Mockus} = \frac{2.08 \times A \times P_{EST} \times C}{\sqrt{t_C} + 0.6 \times t_C} \quad (19)$$

where
Q_{Mockus} = the peak flow rate according to Mockus (m^3/s);
A = the area of the watershed (km^2);
P_{EST} = the estimated level of precipitation (cm);
C = the coefficient of surface runoff (Table A2);
t_C = the concentration time (hours).

In order to guarantee that the population is secure, the dimensions of hydraulic structures have to consider a fill rate below 85% [55,57]. Hence, the implementation of mechanisms that enable the regulation of the runoff—for instance, spillways—assumes a significant level of importance.

As mentioned above, Equation (20) was used to calculate the fill rate. If the discharge point has insufficient drainage capacity to deal with the level of rainflow that exists in the watershed and cannot ensure that the safety margin is accomplished, it becomes necessary to estimate the dimensions of accurate structures of mitigation, such as detention basins.

$$FR = \frac{Q_P}{Q_M} \times 100 \quad (20)$$

where
FR = the fill Rate (%);
Q_P = each methodology's peak flow rate (m^3/s);
Q_M = the stream discharge point's drainage capacity (m^3/s).

The fill rate is related to a given section's drainage capacity assuming a certain flow. Therefore, in a scenario where this parameter is greater than 100%, the section is not capable of dealing with such a high level of water, which ultimately leads to overflow [57].

2.6. Detention Basin Sizing

In scenarios where the discharge point is not capable of handling the volume of rainwater, it is necessary to design a spillway in order to guarantee the flow's normalization—an important aspect, considering that this flow will ultimately reach the stream's discharge point. In this case, a spillway of the Cipolletti type was picked due to its capacity for facilitating the runoff and reducing turbulence in the areas where there is contact with water [56,59]. Its dimensions were calculated using Equation (21).

Once the flow to be drained to the discharge point has been established and regulated, it becomes possible to calculate the level of water that the detention basin will retain. To determine this level of water, two approaches were considered: the Dutch method, and the simplified triangular hydrograph (STH) (Equations (22) and (23), respectively).

$$Q_S = 1.86 \times L_{SD} \times H_D{}^{1.5} \quad (21)$$

where
Q_S = the flow drained by the spillway (m^3/s);
L_{SD} = the sill's width (m^3/s);
H_D = the height of the waterline above the sill (m).

$$V_A = (Q_P - Q_S) \times t_C \times 3600 \quad (22)$$

$$V_A = \frac{(Q_P - Q_S) \times (2 \times t_C - 2 \times [Q_S / \{Q_P / t_C\}])}{2} \quad (23)$$

where
V_A = the volume of storage (m^3);
Q_P = each methodology's peak flow rate (m^3/s);
Q_S = the flow drained by the spillway (m^3/s);
t_C = the concentration time (hours).

It should be noted that the basis for Equation (23) can be found in the geometric examination that was conducted based on the STH approach (Figure A1). Indeed, this equation was established by taking into account an event that lasts at least twice as long as a watershed's concentration time. Considering that the last particle of rainwater to reach the stream's discharge point would come from the farthest point and would be generated in the last moment of the precipitation event, it becomes clear that it would be necessary to consider the value of the concentration time for the volume drained by the river's discharge point [57].

Given that the Dutch method fails to account for the damping and delay of the precipitation hydrograph, the hydraulic structures whose dimensions are estimated considering this methodology might end up being oversized [60], as demonstrated in Figure 4, where q_s is the spillway's runoff capacity, t_c is the concentration time, t_{MAX} is the maximum duration of precipitation (base), t_d is the delay associated with the beginning of the process of accumulation of water in the detention basin, $H_{a,MAX}$ is the maximum capacity of storage, and $i(t_{MAX})$ is the intensity of precipitation associated with the maximum duration.

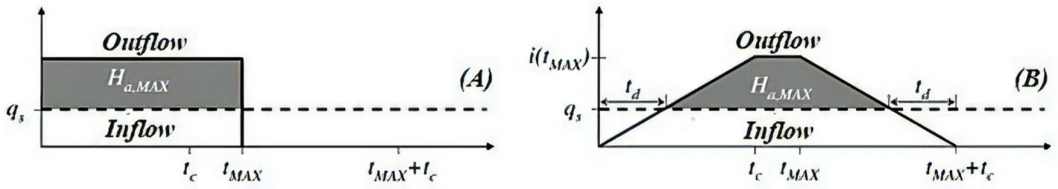

Figure 4. (**A**) Dutch method; (**B**) STH method (source: [27]).

Thus, it was demonstrated that, when resorting to the Dutch method, the storage process and precipitation initiate at the same time, which is an unrealistic scenario, given that storage will not begin until the moment when the downstream-drained flow exceeds the runoff capacity of the spillway.

2.7. Modification of the Roughness Coefficient

Additionally, from a structural perspective, as a mitigation strategy, the alteration of the roughness coefficient of the watercourse's riverbed and walls was considered. One of the most significant advantages associated with this measure is the fact that it enhances the drainage capacity by diminishing the friction level. In terms of the Manning–Strickler equation, this measure can be seen as a modification of the value associated with the "n" parameter, aiming to enhance a certain watercourse's flow, which might be accomplished by changing the material that covers the stream's riverbed and walls [57].

3. Results

Regarding the results presented in this section, it is relevant to note that these values were obtained by resorting to the aforementioned formulae. Furthermore, an analysis of each of the indicators presented in Table 1 was conducted in order to study the characteristics of this watershed's main watercourse, from a morphometric perspective. These indicators were later correlated with reference values from different sources.

Table 1. Parameters calculated or extracted from ArcGIS.

Parameter	Measurement Unit	Result
Area	km^2	14.653
Perimeter	km	31.640
Main Watercourse's Length	km	12.370
Main Watercourse's Maximum Height	m	1660.060
Main Watercourse's Minimum Height	m	0.000
Average Concentration Time	Hours	1.845
Gravelius Coefficient of Compactness	Dimensionless	2.332
Elongation Factor	Dimensionless	15.025
Shape Factor	Dimensionless	0.153
Number of Watercourses	Units	475.000
Average Bifurcation Ratio	Dimensionless	4.567
Strahler Classification	Dimensionless	5.000

First, the analysis focused on the watershed's area, as this parameter has significant importance in studying the volume drained to the stream's discharge point. Considering its area, a watershed might be characterized as follows: very large > 20 km^2; large > 10 km^2; medium > 1 km^2; small < 1 km^2 [61]. In this case, the São João watershed (Funchal) can be classified as "Large", which can be translated into a higher recurrence of floods. Nonetheless, it is worth noting that the reference values presented here are arbitrary and, therefore, might end up differing depending on the type of study that is being undertaken [61].

When comparing the altitudes of this watershed's borders and central region, as illustrated in Figure 5, one could point out that the borders generally present higher altitudes. Hence, this characteristic contributes to a rapid supply of water to the main

watercourse, which means that the flow in the stream and, ultimately, in the discharge point will be larger.

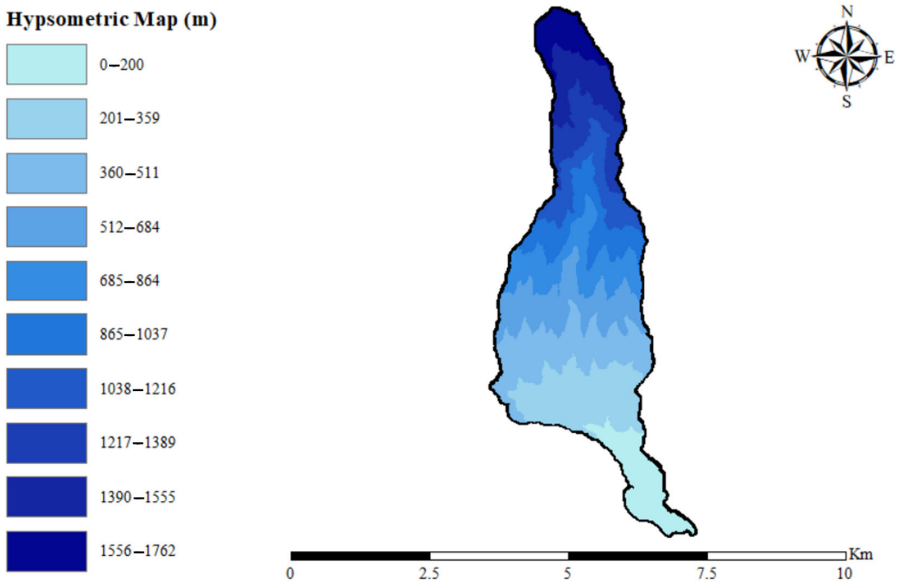

Figure 5. Hypsometric map—DEM file (source: authors, using ESRI ArcGIS, 2020).

As Figure 6 demonstrates, this watershed has various low- and medium-order watercourses supplying the main one, indicating a high drainage capacity. Indeed, the hydrological behavior of a given region can be studied through the hydric density index. This parameter expresses a region's tendency to generate new channels. Thus, watersheds that possess higher levels of hydric density are prone to having numerous ephemeral channels [57].

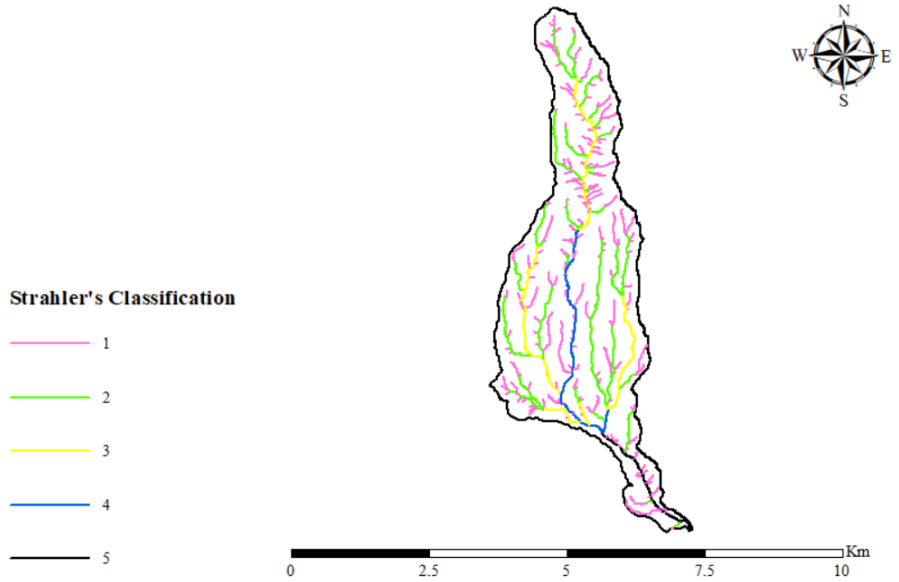

Figure 6. Strahler classification (source: authors, using ESRI ArcGIS, 2020).

Considering the data that were made available by the SNIRH, it became possible to study the precipitation [62]. In fact, we considered sample data that encompassed a period of 16 years, as shown in Table A4 and Figure A2. The results listed in Table 2 were obtained by resorting to a Gumbel-distribution-based probabilistic processing.

Then, when the intensity of precipitation had already been estimated, considering a 100-year return period, the peak flow rates were calculated based on the methods presented in the previous section, as displayed in Table 3. Given that the study region is located in a peripheral area with a significant presence of commercial buildings, in the Rational methodology, the coefficient associated with surface drainage was found to be 0.500 (Table 4). This coefficient represents the proportion of water that is expected to be drained superficially—in this case, approximately half of the volume of water is expected to drain superficially.

Table 2. Precipitation parameters.

Parameter	Symbol	Measurement Unit	Result
Average Annual Precipitation	P_M	mm	95.900
Standard Deviation	S'	mm	51.865
Frequency Factor	K_T	Dimensionless	3.136
Coefficient of Time Distribution	k	Dimensionless	0.420
Maximum Annual Daily Precipitation	P_{EST}	mm	284.309
Precipitation Intensity	I	mm/h	119.306

Table 3. Peak flow rate.

Methodology	Flow (m^3/s)
Forti	185.155
Rational	234.489
Giandotti	211.086
Mockus	239.941

Table 4. Surface drainage coefficient adopted (source: [63]).

Urban Areas		
Occupation of the Land		**Coefficient of Surface Drainage**
Commercial Area	City Center	0.700–0.950
	Peripheral Areas	**0.500**–0.700

In terms of the reduction coefficient (λ), the value that was chosen to estimate the flow through the methodology suggested by Giandotti can be seen in Table 5.

Table 5. Adopted Giandotti reduction coefficient (source: [64]).

Area (km^2)	λ	Equivalent "C"
<300	0.346	1.250

The Manning–Strickler equation was utilized to analyze the stream discharge point's drainage capacity; the results derived from this equation can be found in Table 6. Moreover, this equation allows for a more accurate analysis of whether this watershed's discharge point would require the implementation of a detention basin. Given that the stream's walls and bed presented distinct roughness coefficients, it became necessary to resort to a weighted mean considering these two coefficients. On the one hand, the walls are in good condition—and, therefore, n = 0.020; on the other hand, the riverbed's surface has the presence of sediments and vegetation, which implies that, in comparison to the walls, it presents a poorer state of conservation (n = 0.040). Additionally, it is worth noting that the slope in the region of the stream's discharge point is significantly low, and this ends up contributing to a decrease in terms of the flow's velocity and the section's drainage capacity. Thus, to consider a critical scenario, a slope of 0.01 m/m was considered for the reference section.

Table 6. Assessment of the need for detention basin implementation.

Parameter	Measurement Unit	Result
Stream Discharge Point's Width	m	10.000
Stream Discharge Point's Height	m	4.000
Stream Discharge Point's Drainage Capacity	m^3/s	218.946
Fill Rate—Forti (before Regularization)	%	85
Fill Rate—Rational (before Regularization)	%	107
Fill Rate—Giandotti (before Regularization)	%	96
Fill Rate—Mockus (before Regularization)	%	110

Considering that the Fill Rate surpassed the predefined level of 85% for three of the four methodologies adopted—Giandotti, Mockus, and Rational—it was found to be necessary to implement mitigation measures, namely, a detention basin. Thus, the dimensions of the detention basin were estimated taking into account the flows previously obtained, in addition to the existing spatial and urban limitations due to the presence of infrastructure in the stream's surroundings.

To calculate the detention basin's appropriate dimensions, first, it was necessary to size a Cipolletti trapezoid spillway, since this would enable the flow's regularization and control. As a result, the spillway's characteristics are listed in Table 7.

Table 7. Application of the Cipolletti spillway.

Parameter	Measurement Unit	Result
Spillway's Width	m	8.000
Height of the Spillway Sill	m	4.00
Outflow of the Spillway	m^3/s	119.040
Fill Rate—Rational (after Regularization)	%	54
Fill Rate—Giandotti (after Regularization)	%	54
Fill Rate—Mockus (after Regularization)	%	54

Then, in a second stage, both the Dutch method and the STH method were utilized to size the detention basin. However, due to the fact that these two methods are relatively simplified, using them might lead to oversized structures. In addition, this structure's height and width were defined as identical to the existing cross-section, aiming to diminish the impacts of the implementation of a detention basin from both the environmental and urban perspectives. The sole remaining variable was its length, which should not be larger than the main channel's length.

Table 8 presents the dimensions obtained through the Dutch method and the STH method regarding this structure.

Table 8. Detention basin sizing.

Parameter	Measurement Unit	Result
Width	m	10.000
Height	m	4.000
Length—Dutch Method (Rational)	m	19,170.306
Length—STH Method (Rational)	m	9438.365
Length—Dutch Method (Giandotti)	m	15,284.238
Length—STH Method (Giandotti)	m	6664.833
Length—Dutch Method (Mockus)	m	10,115.659
Length—STH Method (Mockus)	m	20,075.611

Lastly, altering the roughness coefficient without changing the riverbed's vegetation was seen as a substitute approach to mitigate the impact of these events. As such, the values presented in Table 9 are related to the enhancement of the riverbed's level of conservation, which is expected to lead to a decrease in terms of friction and, consequently, to an increase in the stream's drainage capacity.

Table 9. Modification of the roughness coefficient.

Parameter	Measurement Unit	Result
Roughness Coefficient of the Wall—Modified	$m^{-1/3}$	0.012
Roughness Coefficient of the Riverbed—Modified	$m^{-1/3}$	0.030
Stream Discharge Point's Drainage Capacity—Modified	m^3/s	309.620
Fill Rate—Rational (after Modification)	%	76
Fill Rate—Giandotti (after Modification)	%	68
Fill Rate—Mockus (after Modification)	%	77

The wall's revised roughness coefficient refers to a concrete-finished surface that presents a satisfying level of conservation, while the riverbed's sedimentation and vegetation are maintained. Table 10 presents a summary of the coefficients utilized.

Table 10. Adopted roughness coefficients (source: [64]).

Typology of the Channel	Very Good	Good	Regular	Bad
Channel with a Vegetated and Stony Slope	0.025	**0.030**	0.035	0.040
Concrete-Finished Surface	0.011	**0.012**	0.013	0.015

4. Discussion

This study's main goal was to evaluate the need for simplified mitigation measures regarding flooding events in the São João watershed (Funchal). When it was demonstrated that this watershed required such measures, the implementation of a detention basin—a structural measure—was efficient in regulating the volume of water at the stream's discharge point [57]. In fact, while the fill rate obtained through three of the four methodologies utilized—Giandotti, Mockus, and Rational—was initially above 85% (107%, 96%, and 110%, respectively), it fell to a far more satisfying value as a result of the detention basin (54%—a value that is in line with the safety margin that had been pre-established). Additionally, this study's findings are in line with the flood risk assessments carried out by the Regional Directorate for Territorial Ordering and Environment (DROTA), as demonstrated in Table 11, thereby demonstrating that this study presents a satisfying level of accuracy.

Table 11. Watersheds with high flood risk (source: [65]).

Municipality	Watershed
Funchal	João Gomes Santa Luzia São João Ribeiro Seco Ribeiro da Nora Ribeiro do Lazareto

This study also focused on provoking the fewest possible alterations in the surrounding areas of the stream, as preserving natural elements and values in urban regions in currently considered to be a relevant requirement for the environmental revitalization of these areas [66]. Furthermore, ensuring that urban and natural systems harmoniously coexist is key to accomplishing the goal of sustainability [67,68]. Conversely, an unorganized process of urbanization might create urban voids [69].

It was therefore concluded that both the width and height of the streams should not be altered, which ultimately resulted in length being the sole existing variable. Given this assumption, despite the Dutch method presenting efficient results in terms of the regularization of the flow, it cannot be applied because it would require an alteration of either the height or width, given that this structure's length was larger than the main waterway's.

Identical restraints were considered with regard to the STH method. In this case, when comparing the two lengths, the detention basin's value did not surpass the one presented by the main waterway, meaning that the methodology was applicable.

Regarding the modification that was suggested for the stream's roughness coefficient, it was determined to only improve its conservation level, which means that the riverbed's vegetated and stony characteristics would be maintained, as completely removing all of the sediments and vegetation would be a complex, recurrent, and costly process. In terms of the walls, frequent maintenance should not be needed, considering that abrasion-induced wear would only take place in alluvial channels that drain substantial volumes of water and sizable sediments.

Even though it was a simplified measure, modifying the stream's roughness coefficient can be seen as an effective strategy, since it allows the discharge point to operate below the predetermined filling limit. Additionally, it is worth noting that this measure and the STH method can be applied simultaneously, resulting in a detention basin that would not demand such a large length.

Still, it is important to note that the methodologies mentioned above are relatively simplified—that is, they do not consider local specificities. As a result, the outcomes have a significant safety margin incorporated, leading to oversized structures.

5. Conclusions

This study's findings indicate that the São João watershed (Funchal) is vulnerable to flooding events, especially when extreme levels of precipitation occur; indeed, such vulnerability is also noted in DROTA's Flood Risk Report. This scenario occurs due to the stream bed's characteristics—namely, the fact that its surface has sediments and vegetation, which end up diminishing the flow's velocity and the stream's drainage capacity. This is particularly true for areas that have a very reduced slope—namely, the stream discharge point. In fact, the deficient drainage capacity that this watershed's discharge point possesses is supported by three of the four methodologies that were used—Giandotti, Mockus, and Rational.

In terms of the mitigation strategies, the Dutch method had no applicability, as it demanded an excessive length for the detention basin—even larger than the main watercourse's length. In contrast, the STH method brings more adequate results, as it allows this structure to be implemented without modifying the stream's height or width.

Lastly, the alteration proposed regarding the roughness coefficient also proved to be efficient. Among the advantages that this strategy possesses is the fact that it is a relatively simple measure to implement.

Given the impossibility of addressing all of the aspects that constitute a more extensive and effective study in this case, further research could be conducted to complement or improve the findings presented here—for instance, studying the drainage capacity associated with the existing urban hydraulic system, aiming to diminish the volume stored in detention basins; analyzing the deposition of sediments considering the main watercourse's entrainment velocity [70]; monitoring the artificial channels' walls' deterioration levels, as a result of abrasion, and analyzing the maximum amount of time to go ahead with maintenance (for instance, desilting and silting processes); studying how the artificial channels' processes of degradation can be correlated with the tributaries' water quality [71,72]; analyzing the impact of urbanization on the increase of the flow; planning and estimating the costs associated with the adoption of the mitigation strategies suggested in the present study; studying the impact of tide levels on the drainage capacity of artificial water channels and the probability associated with flooding events in the area of the stream's discharge point; and studying the impact of this type of channel from the perspective of territorial planning and management—i.e., how they can be adapted to watersheds located in rural areas.

The findings of this study are consistent with the results and outcomes suggested in analogous studies that also considered case studies and simulations as catalysts for scientific advancement [73,74]

Author Contributions: Conceptualization, S.L., R.A., M.F. and L.G.; methodology, S.L.; software, S.L. and L.G.; validation, S.L. and L.G.; formal analysis, S.L. and L.G.; investigation, S.L.; resources, L.G.; data curation, S.L. and L.G.; writing—original draft preparation, S.L., R.A., M.F. and L.G.; writing—review and editing, S.L.; visualization, R.A., M.F. and L.G.; supervision, R.A., M.F. and L.G.; project administration, S.L. All authors have read and agreed to the published version of the manuscript.

Funding: Through the funding provided by MÁXIMA DINÂMICA REPARAÇÕES E CONSTRUÇÕES LDA and DANIEL SILVA SANTOS UNIP LDA, we were able to obtain the necessary resources to conduct the research, analyze relevant data, and draft this article. Furthermore, their trust and investment in our work demonstrate the recognition of the value and potential of this research. We hope that this enduring partnership continues to promote research and development in the field of civil construction. Once again, we are deeply grateful to MÁXIMA DINÂMICA REPARAÇÕES E CONSTRUÇÕES LDA and DANIEL SILVA SANTOS UNIP LDA for their invaluable support.

Institutional Review Board Statement: Not applicable.

Informed Consent Statement: Not applicable.

Data Availability Statement: The data presented in this study are openly available. Moreover, it is possible to contact one of the study's authors.

Acknowledgments: Special thanks are due to MÁXIMA DINÂMICA REPARAÇÕES E CONSTRUÇÕES LDA and DANIEL SILVA SANTOS UNIP LDA, both Civil Construction Companies, for the generous financial support granted, which made this study and article publication possible. Their significant contribution was fundamental to the success of this research project. We would like to express our sincere gratitude to MÁXIMA DINÂMICA REPARAÇÕES E CONSTRUÇÕES LDA and DANIEL SILVA SANTOS UNIP LDA for their continuous support in advancing scientific knowledge within the field of civil construction. Without their sponsorship, this publication would not have been possible.

Conflicts of Interest: The authors declare no conflict of interest.

Appendix A

Table A1. Manning–Strickler roughness coefficients (source: [64]).

Type of Channel and Description	Very Good	Good	Regular	Bad
Mortared Stone Masonry	0.017	0.020	0.025	0.030
Rigged Stone Masonry	0.013	0.014	0.015	0.017
Dry Stone Masonry	0.025	0.033	0.033	0.035
Brick Masonry	0.012	0.013	0.015	0.017
Smooth Metal Gutters (Semicircular)	0.011	0.012	0.013	0.016
Open Channels in Rock (Irregular)	0.035	0.040	0.045	-
Channels with Bottom on Land and Slope with Stones	0.028	0.030	0.033	0.035
Channels with Stony Bed and Vegetated Slope	0.025	0.030	0.035	0.040
Channels with Concrete Coating	0.012	0.014	0.016	0.018
Earth Channels (Rectilinear and Uniform)	0.017	0.020	0.023	0.025
Dredged Canals	0.025	0.028	0.030	0.033
Clay Conduits (Drainage)	0.011	0.012	0.014	0.017
Vitrified Clay Conduits (Sewage)	0.011	0.013	0.015	0.017
Flattened Wooden Plank Conduits	0.010	0.012	0.013	0.014
Gabion	0.022	0.030	0.035	-
Cement Mortar Surfaces	0.011	0.012	0.013	0.015
Smoothed Cement Surfaces	0.010	0.011	0.012	0.013
Cast-Iron -Coated Tube with Tar	0.011	0.012	0.013	-
Uncoated Cast-Iron Pipe	0.012	0.013	0.014	0.015
Brass or Glass Tubes	0.009	0.010	0.012	0.013
Concrete Pipes	0.012	0.013	0.015	0.016
Galvanized Iron Pipes	0.013	0.014	0.015	0.017
Rectilinear and Uniform Clean Streams and Rivers	0.025	0.028	0.030	0.033
Streams and Rivers Cleared Rectilinear and Uniform with Stones and Vegetation	0.030	0.033	0.035	0.040
Streams and Rivers Cleared Rectilinear and Uniform with Intricacies and Wells	0.035	0.040	0.045	0.050
Spread Margins with Little Vegetation	0.050	0.060	0.070	0.080
Spread Margins with Lots of Vegetation	0.075	0.100	0.125	0.150

Table A2. Surface runoff coefficients (source: [27]).

Urban Areas		
Occupation of the Land		**Surface Runoff Coefficient**
Green Areas	Lawns on Sandy Soils	0.050–0.200
	Lawns on Heavy Soils	0.150–0.350
	Parks and Cemeteries	0.100–0.350
	Sports Fields	0.200–0.350
Commercial Areas	City District	0.700–0.950
	Periphery	0.500–0.700
Residential Areas	Town-Center Villas	0.300–0.500
	Villas on the Outskirts	0.250–0.400
	Apartment Buildings	0.500–0.700
Industrial Areas	Dispersed Industry	0.500–0.800
	Concentrated Industry	0.600–0.900
Railways		0.200–0.400
Streets and Roads	Paved	0.700–0.900
	Concrete	0.800–0.950
	In brick	0.700–0.850

Table A3. Giandotti reduction coefficients (source: [64]).

A (km^2)	**λ**	**"C" Equivalent**
<300	0.346	1.250
300–500	0.277	1.000
500–1000	0.197	0.710
1000–8000	0.100	0.360
8000–20,000	0.076	0.270
20,000–70,000	0.055	0.200

Table A4. Historical precipitation data (source: [62]).

n	**Year**	**(mm)**
1	1998/1999	170.000
2	1999/2000	180.700
3	2000/2001	135.000
4	2001/2002	190.000
5	2002/2003	195.400
6	2003/2004	141.000
7	2004/2005	103.200
8	2005/2006	91.400
9	2006/2007	141.400
10	2007/2008	104.600
11	2008/2009	155.000
12	2009/2010	257.800
13	2010/2011	148.400
14	2011/2012	288.600
15	2012/2013	267.400
16	2013/2014	61.200

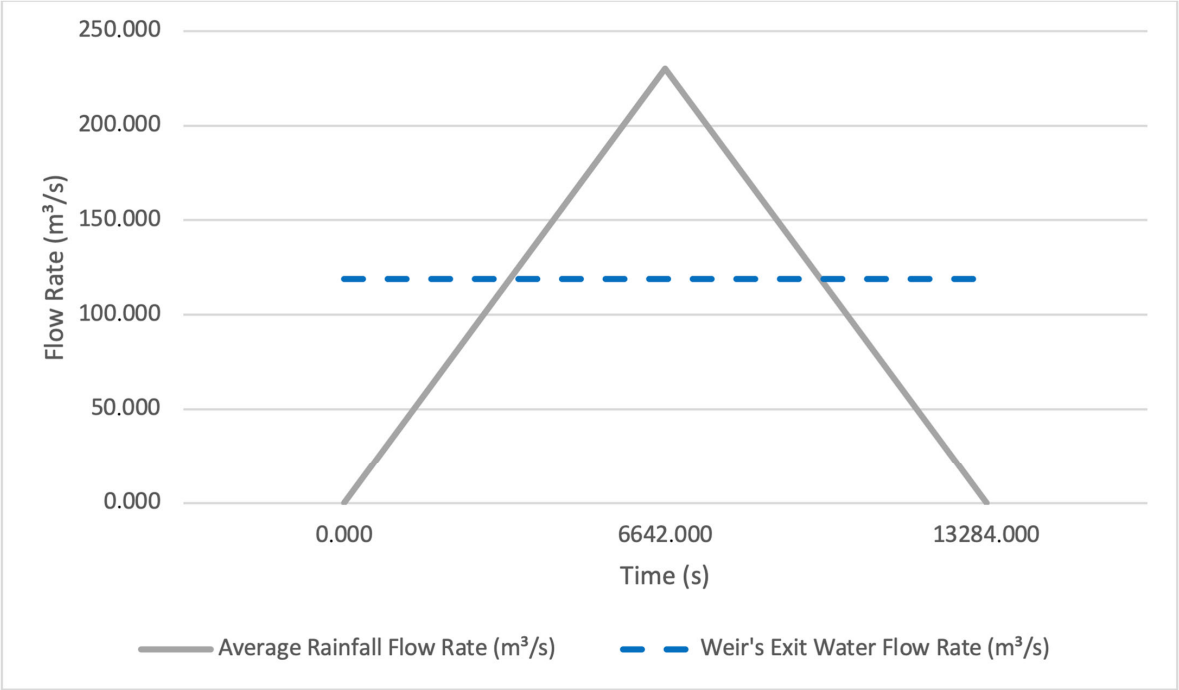

Figure A1. Ternary phase diagram.

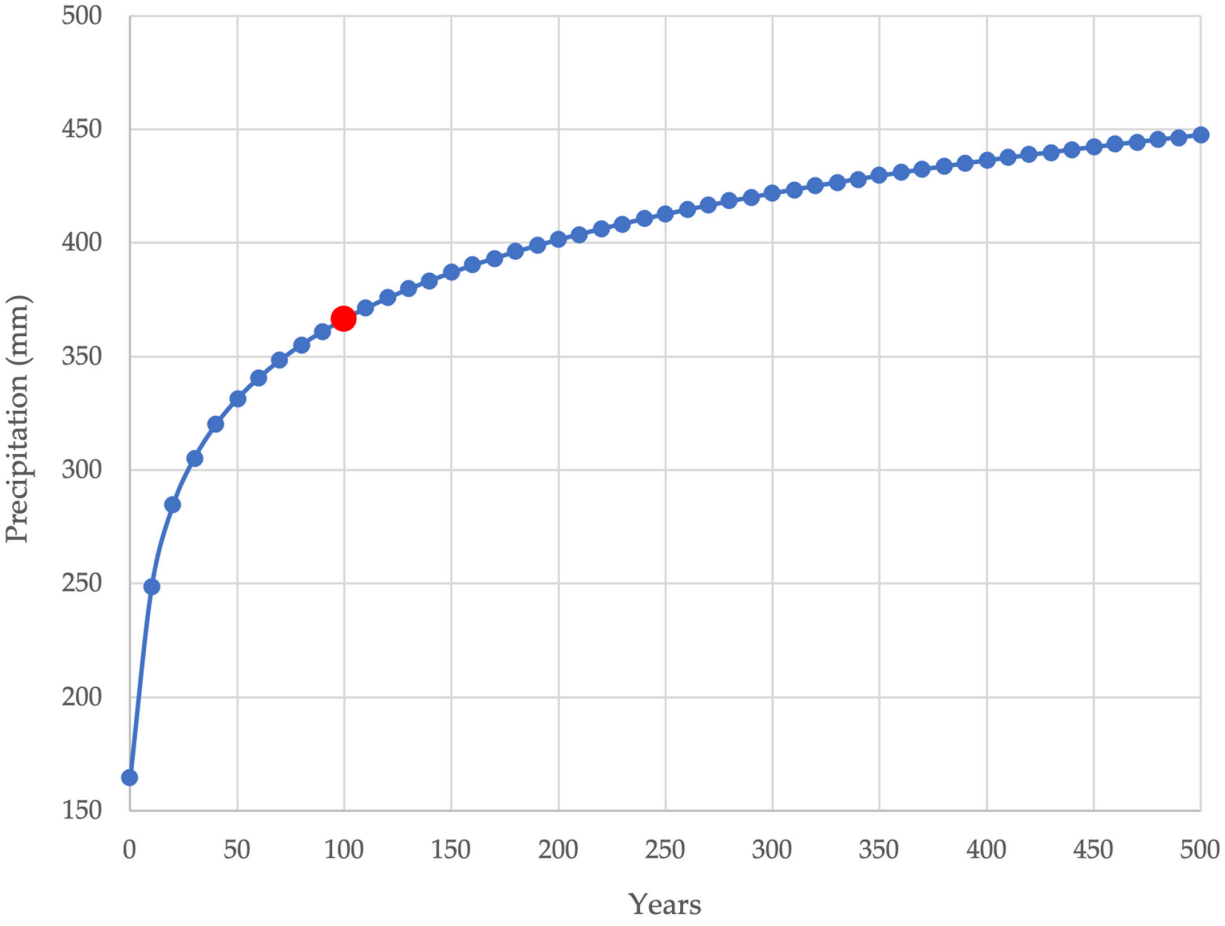

Figure A2. Expected rainfall for São João watershed (Funchal).

References

1. Anwana, E.O.; Owojori, O.M. Analysis of Flooding Vulnerability in Informal Settlements Literature: Mapping and Research Agenda. *Soc. Sci.* **2023**, *12*, 40. [CrossRef]
2. Blöschl, G.; Hall, J.; Viglione, A.; Perdigão, R.A.P.; Parajka, J.; Merz, B.; Lun, D.; Arheimer, B.; Aronica, G.T.; Bilibashi, A.; et al. Changing Climate Both Increases and Decreases European River Floods. *Nature* **2019**, *573*, 108–111. [CrossRef] [PubMed]
3. Janicka, E.; Kanclerz, J. Assessing the Effects of Urbanization on Water Flow and Flood Events Using the HEC-HMS Model in the Wirynka River Catchment, Poland. *Water* **2023**, *15*, 86. [CrossRef]
4. Hassan, M.M. Monitoring Land Use/Land Cover Change, Urban Growth Dynamics and Landscape Pattern Analysis in Five Fastest Urbanized Cities in Bangladesh. *Remote Sens. Appl. Soc. Environ.* **2017**, *7*, 69–83. [CrossRef]
5. Malede, D.A.; Alamirew, T.; Andualem, T.G. Integrated and Individual Impacts of Land Use Land Cover and Climate Changes on Hydrological Flows over Birr River Watershed, Abbay Basin, Ethiopia. *Water* **2023**, *15*, 166. [CrossRef]
6. Modelling Hydrological Response to Different Land-use and Climate Change Scenarios in the Zamu River Basin of Northwest China-Wang-2008-Hydrological Processes-Wiley Online Library. Available online: https://onlinelibrary.wiley.com/doi/10.1002/hyp.6846 (accessed on 10 March 2023).
7. Osei, M.A.; Amekudzi, L.K.; Wemegah, D.D.; Preko, K.; Gyawu, E.S.; Obiri-Danso, K. The Impact of Climate and Land-Use Changes on the Hydrological Processes of Owabi Catchment from SWAT Analysis. *J. Hydrol. Reg. Stud.* **2019**, *25*, 100620. [CrossRef]
8. Tekleab, S.; Mohamed, Y.; Uhlenbrook, S. Hydro-Climatic Trends in the Abay/Upper Blue Nile Basin, Ethiopia. *Phys. Chem. Earth Parts ABC* **2013**, *61–62*, 32–42. [CrossRef]
9. Kundzewicz, Z.W.; Su, B.; Wang, Y.; Wang, G.; Wang, G.; Huang, J.; Jiang, T. Flood Risk in a Range of Spatial Perspectives—from Global to Local Scales. *Nat. Hazards Earth Syst. Sci.* **2019**, *19*, 1319–1328. [CrossRef]
10. Hamza, M.H.; Saegh, A.M. Flash Flood Risk Assessment Due to a Possible Dam Break in Urban Arid Environment, the New Um Al-Khair Dam Case Study, Jeddah, Saudi Arabia. *Sustainability* **2023**, *15*, 1074. [CrossRef]
11. Kundzewicz, Z.W.; Schellnhuber, H.-J. Floods in the IPCC TAR Perspective. *Nat. Hazards* **2004**, *31*, 111–128. [CrossRef]
12. Milly, P.C.D.; Wetherald, R.T.; Dunne, K.A.; Delworth, T.L. Increasing Risk of Great Floods in a Changing Climate. *Nature* **2002**, *415*, 514–517. [CrossRef]
13. Gambardella, C.; Parente, R.; Scotto di Santolo, A.; Ciaburro, G. New Digital Field of Drawing and Survey for the Automatic Identification of Debris Accumulation in Flooded Areas. *Sustainability* **2023**, *15*, 479. [CrossRef]
14. Gaur, S.; Mittal, A.; Bandyopadhyay, A.; Holman, I.; Singh, R. Spatio-Temporal Analysis of Land Use and Land Cover Change: A Systematic Model Inter-Comparison Driven by Integrated Modelling Techniques. *Int. J. Remote Sens.* **2020**, *41*, 9229–9255. [CrossRef]
15. Gaur, S.; Bandyopadhyay, A.; Singh, R. Projecting Land Use Growth and Associated Impacts on Hydrological Balance through Scenario-Based Modelling in the Subarnarekha Basin, India. *Hydrol. Sci. J.* **2021**, *66*, 1997–2010. [CrossRef]
16. Gaur, S.; Singh, R. A Comprehensive Review on Land Use/Land Cover (LULC) Change Modeling for Urban Development: Current Status and Future Prospects. *Sustainability* **2023**, *15*, 903. [CrossRef]
17. Flood Inundation Assessment for the Hanoi Central Area, Vietnam under Historical and Extreme Rainfall Conditions | Scientific Reports. Available online: https://www.nature.com/articles/s41598-018-30024-5 (accessed on 10 March 2023).
18. Du, W.; FitzGerald, G.J.; Clark, M.; Hou, X.-Y. Health Impacts of Floods. *Prehospital Disaster Med.* **2010**, *25*, 265–272. [CrossRef]
19. Norel, M.; Krawiec, K.; Kundzewicz, Z.W. Machine Learning Modeling of Climate Variability Impact on River Runoff. *Water* **2021**, *13*, 1177. [CrossRef]
20. Mrozik, K.D. Problems of Local Flooding in Functional Urban Areas in Poland. *Water* **2022**, *14*, 2453. [CrossRef]
21. Kvočka, D.; Falconer, R.A.; Bray, M. Flood Hazard Assessment for Extreme Flood Events. *Nat. Hazards* **2016**, *84*, 1569–1599. [CrossRef]
22. Morrison, A.; Westbrook, C.J.; Noble, B.F. A review of the flood risk management governance and resilience lit-erature. *J. Flood Risk Manag.* **2018**, *11*, 291–304. [CrossRef]
23. Dordi, T.; Henstra, D.; Thistlethwaite, J. Flood Risk Management and Governance: A Bibliometric Review of the Literature. *J. Flood Risk Manag.* **2022**, *15*, e12797. [CrossRef]
24. O'Donnell, E.C.; Thorne, C.R. Drivers of Future Urban Flood Risk. *Philos. Trans. R. Soc. Math. Phys. Eng. Sci.* **2020**, *378*, 20190216. [CrossRef]
25. Arduino, G.; Reggiani, P.; Todini, E. Recent Advances in Flood Forecasting and Flood Risk Assessment. *Hydrol. Earth Syst. Sci.* **2005**, *9*, 280–284. [CrossRef]
26. Zanchetta, A.D.L.; Coulibaly, P. Recent Advances in Real-Time Pluvial Flash Flood Forecasting. *Water* **2020**, *12*, 570. [CrossRef]
27. Delrieu, G.; Nicol, J.; Yates, E.; Kirstetter, P.E.; Creutin, J.D.; Anquetin, S.; Obled, C.; Saulnier, G.-M.; Ducrocq, V.; Gaume, E.; et al. The Catastrophic Flash-Flood Event of 8–9 September 2002 in the Gard Region, France: A First Case Study for the Cévennes–Vivarais Mediterranean Hydrometeorological Observatory. *J. Hydrometeorol.* **2005**, *6*, 34–52. [CrossRef]
28. Gaume, E.; Livet, M.; Desbordes, M.; Villeneuve, J.-P. Hydrological Analysis of the River Aude, France, Flash Flood on 12 and 13 November 1999. *J. Hydrol.* **2004**, *286*, 135–154. [CrossRef]
29. Haynes, K.; Coates, L.; van den Honert, R.; Gissing, A.; Bird, D.; Dimer de Oliveira, F.; D'Arcy, R.; Smith, C.; Radford, D. Exploring the Circumstances Surrounding Flood Fatalities in Australia—1900–2015 and the Implications for Policy and Practice. *Environ. Sci. Policy* **2017**, *76*, 165–176. [CrossRef]

30. Vinet, F.; Lumbroso, D.; Defossez, S.; Boissier, L. A Comparative Analysis of the Loss of Life during Two Recent Floods in France: The Sea Surge Caused by the Storm Xynthia and the Flash Flood in Var. *Nat. Hazards* **2012**, *61*, 1179–1201. [CrossRef]
31. Allaire, M. Socio-Economic Impacts of Flooding: A Review of the Empirical Literature. *Water Secur.* **2018**, *3*, 18–26. [CrossRef]
32. Merz, B.; Blöschl, G.; Vorogushyn, S.; Dottori, F.; Aerts, J.C.J.H.; Bates, P.; Bertola, M.; Kemter, M.; Kreibich, H.; Lall, U.; et al. Causes, Impacts and Patterns of Disastrous River Floods. *Nat. Rev. Earth Environ.* **2021**, *2*, 592–609. [CrossRef]
33. Iqbal, U.; Perez, P.; Li, W.; Barthelemy, J. How Computer Vision Can Facilitate Flood Management: A Systematic Review. *Int. J. Disaster Risk Reduct.* **2021**, *53*, 102030. [CrossRef]
34. Iqbal, U.; Riaz, M.Z.B.; Barthelemy, J.; Hutchison, N.; Perez, P. Floodborne Objects Type Recognition Using Computer Vision to Mitigate Blockage Originated Floods. *Water* **2022**, *14*, 2605. [CrossRef]
35. Arshad, B.; Ogie, R.; Barthelemy, J.; Pradhan, B.; Verstaevel, N.; Perez, P. Computer Vision and IoT-Based Sensors in Flood Monitoring and Mapping: A Systematic Review. *Sensors* **2019**, *19*, 5012. [CrossRef]
36. Nofal, O.M.; van de Lindt, J.W. High-Resolution Flood Risk Approach to Quantify the Impact of Policy Change on Flood Losses at Community-Level. *Int. J. Disaster Risk Reduct.* **2021**, *62*, 102429. [CrossRef]
37. Abdel-Mooty, M.N.; Yosri, A.; El-Dakhakhni, W.; Coulibaly, P. Community Flood Resilience Categorization Framework. *Int. J. Disaster Risk Reduct.* **2021**, *61*, 102349. [CrossRef]
38. Wasko, C.; Nathan, R.; Stein, L.; O'Shea, D. Evidence of Shorter More Extreme Rainfalls and Increased Flood Variability under Climate Change. *J. Hydrol.* **2021**, *603*, 126994. [CrossRef]
39. Mondal, M.S.H. The Implications of Population Growth and Climate Change on Sustainable Development in Bangladesh. *Jàmbá J. Disaster Risk Stud.* **2019**, *11*, 10. [CrossRef] [PubMed]
40. Iqbal, U.; Riaz, M.Z.B.; Zhao, J.; Barthelemy, J.; Perez, P. Drones for Flood Monitoring, Mapping and Detection: A Bibliometric Review. *Drones* **2023**, *7*, 32. [CrossRef]
41. Frequency Analysis of Monthly Runoff in Intermittent Rivers | World Environmental and Water Resources Congress 2017. Available online: https://ascelibrary.org/doi/10.1061/9780784480625.030 (accessed on 10 March 2023).
42. Khan, Z.; Rahman, A.; Karim, F. An Assessment of Uncertainties in Flood Frequency Estimation Using Bootstrapping and Monte Carlo Simulation. *Hydrology* **2023**, *10*, 18. [CrossRef]
43. Lousada, S.; Gonçalves, L.; Atmaca, A. Hydraulic Planning in Insular Urban Territories: The Case of Madeira Island—São Vicente. *Water* **2022**, *14*, 112. [CrossRef]
44. Apel, H.; Aronica, G.T.; Kreibich, H.; Thieken, A.H. Flood Risk Analyses—How Detailed Do We Need to Be? *Nat. Hazards* **2009**, *49*, 79–98. [CrossRef]
45. Directive 2007/60/EC of the European Parliament and of the Council on the Assessment and Management of Flood Risks—European Environment Agency. Available online: https://www.eea.europa.eu/policy-documents/directive-2007-60-ec-of (accessed on 14 March 2023).
46. Hirabayashi, Y.; Mahendran, R.; Koirala, S.; Konoshima, L.; Yamazaki, D.; Watanabe, S.; Kim, H.; Kanae, S. Global Flood Risk under Climate Change. *Nat. Clim. Change* **2013**, *3*, 816–821. [CrossRef]
47. Birkholz, S.; Muro, M.; Jeffrey, P.; Smith, H.M. Rethinking the Relationship between Flood Risk Perception and Flood Management. *Sci. Total Environ.* **2014**, *478*, 12–20. [CrossRef] [PubMed]
48. Winsemius, H.C.; Aerts, J.C.J.H.; van Beek, L.P.H.; Bierkens, M.F.P.; Bouwman, A.; Jongman, B.; Kwadijk, J.C.J.; Ligtvoet, W.; Lucas, P.L.; van Vuuren, D.P.; et al. Global Drivers of Future River Flood Risk. *Nat. Clim. Chang.* **2016**, *6*, 381–385. [CrossRef]
49. Oliva, A.; Olcina, J. Floods and Emergency Management: Elaboration of Integral Flood Maps Based on Emergency Calls (112)—Episode of September 2019 (Vega Baja Del Segura, Alicante, Spain). *Water* **2023**, *15*, 2. [CrossRef]
50. Chakrabortty, R.; Pal, S.C.; Ruidas, D.; Roy, P.; Saha, A.; Chowdhuri, I. Living with Floods Using State-of-the-Art and Geospatial Techniques: Flood Mitigation Alternatives, Management Measures, and Policy Recommendations. *Water* **2023**, *15*, 558. [CrossRef]
51. De França, J.A.P.; de Almeida, A.B. Plano Regional de Água da Madeira Síntese do Diagnóstico e dos Objectivos. Simpósio de Hidráulica e Recursos Hídricos dos Países de Língua Oficial Portuguesa, Cidade da Praia, República de Cabo Verde, 10–12 November 2003; pp. 751–760.
52. Camacho, R.F. Caracterização, Simulação (à Escala) e Modelação do Escoamento em Canais Artificiais: Aplicação a Caso de Estudo. Master's Thesis, Universidade da Madeira, Funchal, Portugal, 2015.
53. Lousada, S.A.N.; Moura, A.D.S.; Gonçalves, L.B. Numerical modelling of the flow rate in artificial water channels: Application to Ribeira Brava's stream. *Rev. Bras. Planej. E Desenvolv.* **2020**, *9*, 39–59. [CrossRef]
54. Lousada, S.; Cabezas, J.; Castanho, R.A.; Gómez, J.M. Hydraulic Planning in Insular Urban Territories: The Case of Madeira Island-Ribeira Brava. *Water* **2021**, *13*, 2951. [CrossRef]
55. Tucci, C.E.M. *Gestão de Águas Pluviais Urbanas*; Universidade Federal do Rio Grande do Sul (UFRGS): Rio Grande do Sul, Brazil, 1993; p. 270.
56. Gonçalves, L.B.; Lousada, S.A.N. Análise Probabilística de Cheias e o Uso de Bacias de Detenção como Medida Mitigadora: Aplicação à Bacia de Santa Luzia. *Rev. Científica Monfragüe Desarro. Resiliente: Extremadura, Spain* **2020**, *13*.
57. Lousada, S.A.N.; Camacho, R.F. *Hidrologia, Recursos Hídricos e Ambiente: Aulas Teóricas*; Universidade da Madeira: Funchal, Portugal, 2018; Volume 1, ISBN 978-989-8805-33-1.
58. Geomorfologia—Antonio Christofoletti.Pdf. Available online: https://toaz.info/doc-view (accessed on 28 March 2022).

59. Vieira, I.; Barreto, V.; Figueira, C.; Lousada, S.; Prada, S. The Use of Detention Basins to Reduce Flash Flood Hazard in Small and Steep Volcanic Watersheds—A Simulation from Madeira Island. *J. Flood Risk Manag.* **2018**, *11*, S930–S942. [CrossRef]
60. David, L.M.; de Carvalho, R.F. Bacias de Retenção para Controlo de Cheias: Reflexão sobre métodos de dimensionamento. Encontro Nacional de Saneamento Básico. UBI: Beira Interior, Portugal, 2008.
61. Beck, H.E.; Bruijnzeel, L.A.; van Dijk, A.I.J.M.; McVicar, T.R.; Scatena, F.N.; Schellekens, J. The Impact of Forest Regeneration on Streamflow in 12 Mesoscale Humid Tropical Catchments. *Hydrol. Earth Syst. Sci.* **2013**, *17*, 2613–2635. [CrossRef]
62. SNIRH > Dados de Base. Available online: https://snirh.apambiente.pt/index.php?idMain=2&idItem=1&objCover=920123704&objSite=920685506 (accessed on 6 March 2023).
63. *Ven-Te Chow Handbook of Applied Hydrology*; McGraw-Hill: New York, NY, USA, 1964.
64. Gonçalves, J.A.V. Caracterização do Coeficiente de Rugosidade e Seu Efeito no Escoamento em Canais Naturais: Simulação e Modelação (à Escala) no Laboratório de Hidráulica: Aplicação às Ribeiras do Funchal. Master's Thesis, Universidade da Madeira, Funchal, Portugal, 2017.
65. Plano de Gestão de Riscos de Inundação Da RAM-PGRI-RAM—Google Drive. Available online: https://drive.google.com/drive/folders/0BxPHHom7Ioe6bUQybkdoY2RvSVE?resourcekey=0-YYBZnl-ByzCMyDd6INwQUg (accessed on 6 March 2023).
66. Castanho, R.A. Evolución del Procedimiento de Planeamiento Urbano en la Península Ibérica y sus Huellas en el Paisaje Urbano, Retos de Futuro. *Rev. Monfrague Desarro. Resiliente* **2017**, *8*, 2340–5457.
67. Fadigas, L. *Urbanismo e Território—As Políticas Públicas | Edições Sílabo*; Edições Sílabo: Lisbon, Portugal, 2015.
68. Loures, L. Planning and Design in Postindustrial Land Transformation: East Bank Arade River, Lagoa-Case Study. Ph.D. Thesis, University of Algarve, Faro, Portugal, 2011.
69. Alexandre Castanho, R.; Lousada, S.; Manuel Naranjo Gómez, J.; Escórcio, P.; Cabezas, J.; Fernández-Pozo, L.; Loures, L. Dynamics of the Land Use Changes and the Associated Barriers and Opportunities for Sustainable Development on Peripheral and Insular Territories: The Madeira Island (Portugal). In *Land Use—Assessing the Past, Envisioning the Future*; Carlos Loures, L., Ed.; IntechOpen: Rijeka, Croatia, 2019; ISBN 978-1-78985-703-0.
70. Yu, B.Y.; Wu, P.; Sui, J.; Ni, J.; Whitcombe, T. Variation of Runoff and Sediment Transport in the Huai River—A Case Study. *J. Environ. Inform.* **2020**, *35*, 138–147. [CrossRef]
71. Shrestha, N.K.; Wang, J. Water Quality Management of a Cold Climate Region Watershed in Changing Climate. *J. Environ. Inform.* **2019**, *35*, 56–80. [CrossRef]
72. Li, Z.; Li, J.J.; Shi, X.P. A Two-Stage Multisite and Multivariate Weather Generator. *J. Environ. Inform.* **2019**, *35*, 148–159. [CrossRef]
73. Nunes, J.M.; Ramos MIras, J.; Pineiro, A.; Loures, L.; Carrasco, C.; Coelho, J.; Loures, A. Concentrations of Available Heavy Metals in Mediterranean Agricultural Soils and Their Relation with Some Soil Selected Properties: A Case Study in Typical Mediterranean Soils. *Sustainability* **2014**, *6*, 9124–9138. [CrossRef]
74. Vargues, P.; Loures, L. Using Geographic Information Systems in Visual and Aesthetic Analysis: The Case Study of a Golf Course in Algarve. *WSEAS Trans. Environ. Dev.* **2008**, *4*, 774–783.